Extended Data Fig. 1

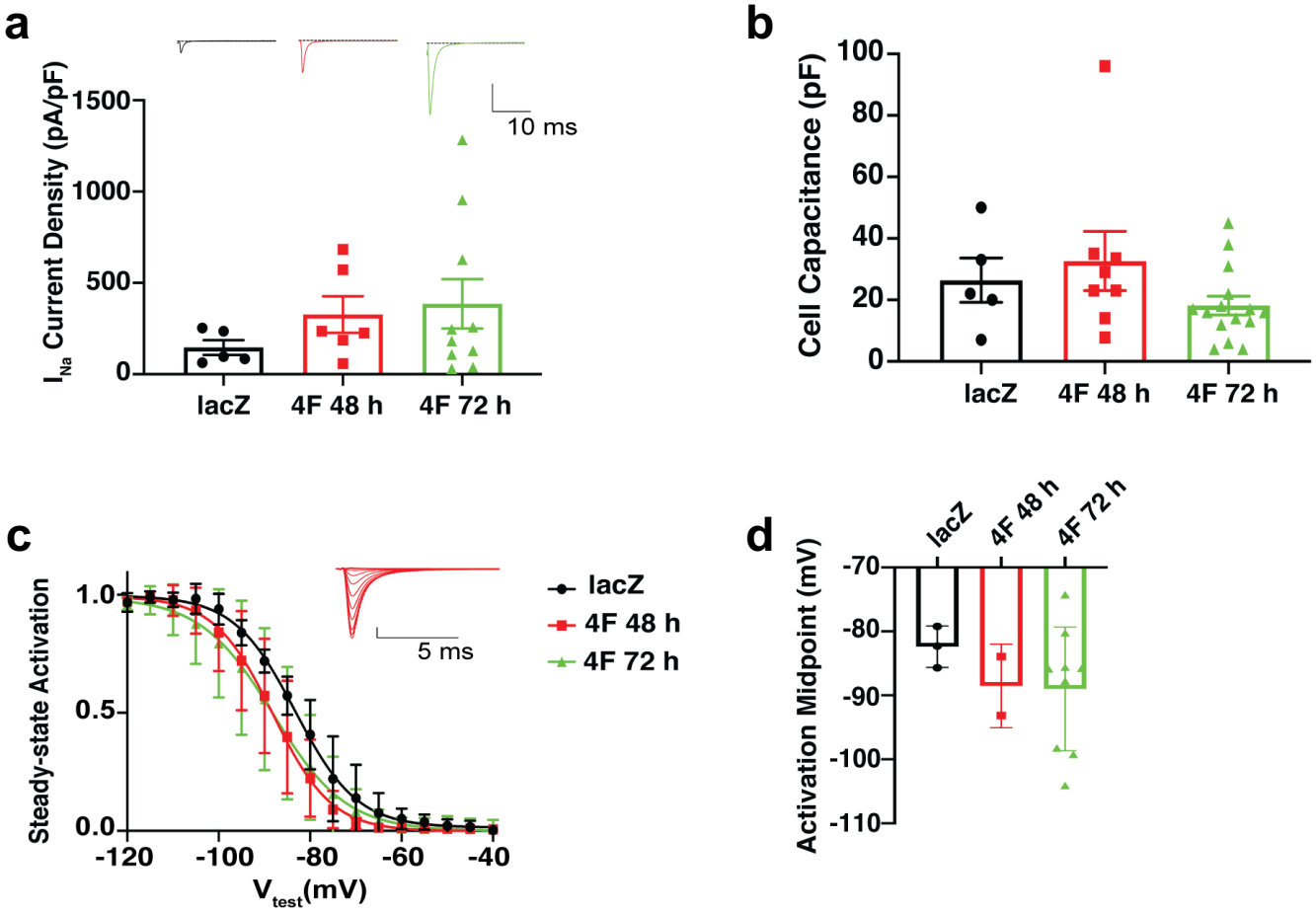

Extended Data Fig. 1. 4F infection of hiPSC-CM does not significantly change I_{Na}. **(a)** Peak I_{Na} current density in lacZ (black), 48 h (red), and 72 h (green) after virus infection with 4F, with exemplar Na^+ current recorded from a V_{hold} 120mV to V_{test} 0mV. Scale bar=0.5 nA/pF, 10 ms. **(b)** Cell capacitance was not different between lacZ, and 4F treated cells either at 48 h or 72 h after infection (Compared to lacZ: 48 h p = 0.74; 72 h p=0.56). **(c)** Inset, a representative family of traces taken at 48 h after infection with 4F. Scale bar: 2 nA, 5 ms. Quantification of the steady-state activation curve demonstrates a trend towards a negative shift of steady-state inactivation midpoint, quantified in **(d).** lacZ: n = 5 cells; 4F 48 h: n = 6 cells; 4F 72 h: n =15 cells.

Extended Data Fig. 2

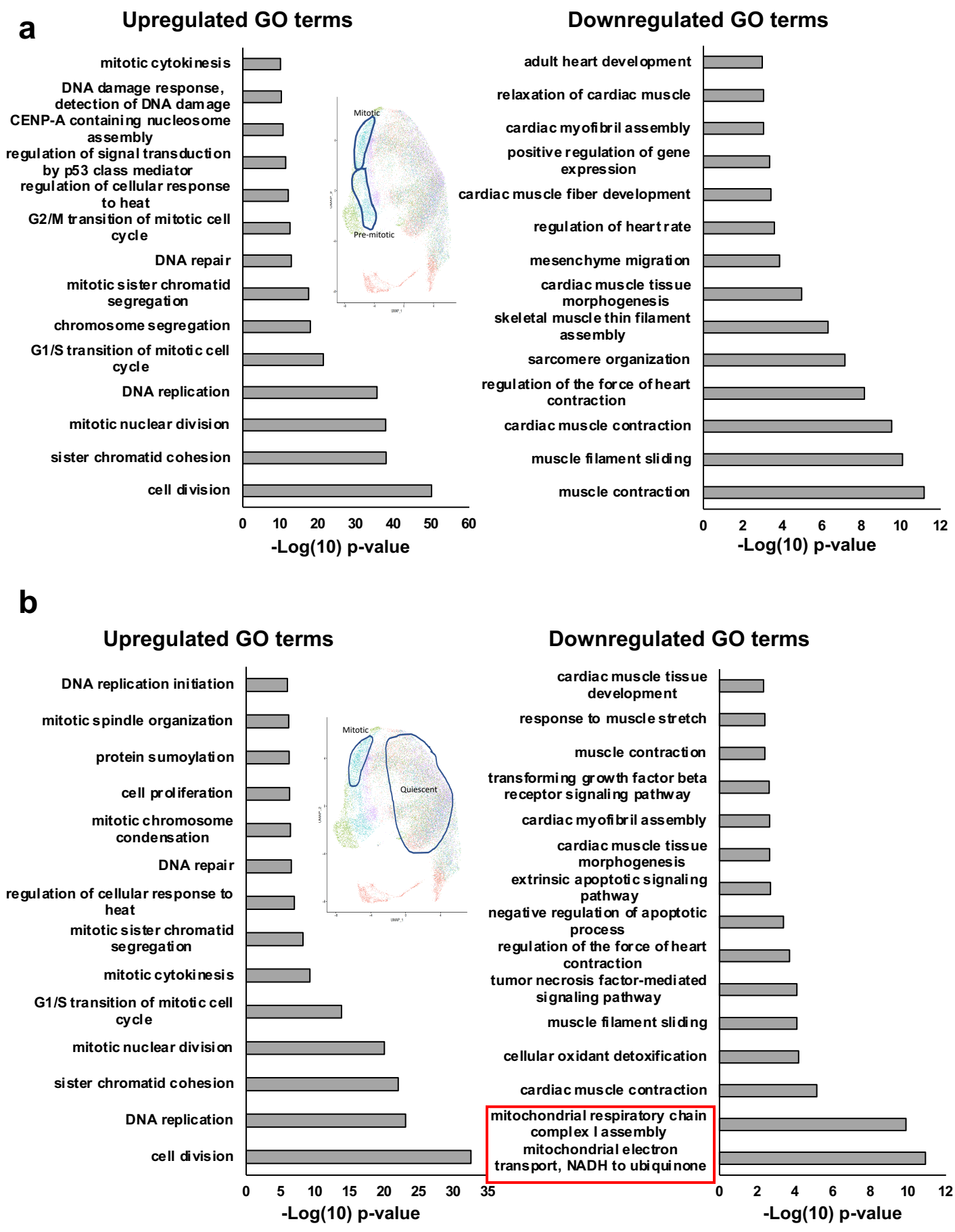

Extended Data Fig. 2. GO terms for differentially expressed genes between mitotic cardiomyocytes and pre-mitotic or quiescent cardiomyocytes 48 h post-infection with 4F.

GO terms for up- and down-regulated genes in the mitotic subpopulation compared with **(a)** the pre-mitotic subpopulation or **(b)** the quiescent subpopulation from the same sample (highlighted in the UMAP plot). Interestingly, the top downregulated GO terms in the mitotic subpopulation compared to the quiescent subpopulation involve mitochondrial electron transport chain genes in addition to the sarcomeric and cardiac contractile genes.

Extended Data Fig. 3

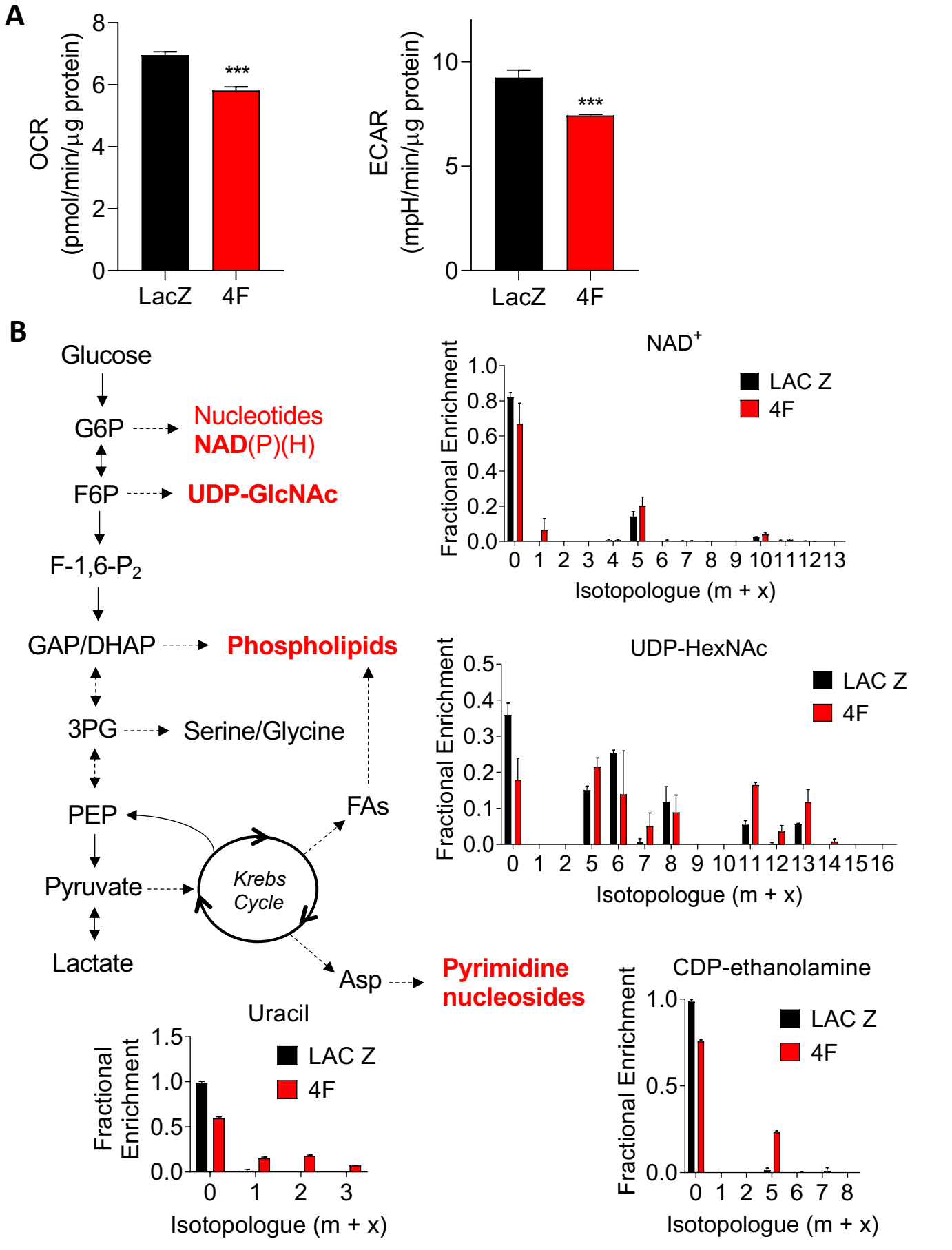

Extended Data Fig. 3. Induction of myocyte proliferation via 4F transduction decreases catabolism and increases anabolism.
(a) Extracellular flux analysis of hiPS-CMs 48 h after transduction with LacZ or 4F adenovirus. Oxygen consumption (OCR); extracellular acidification rate (ECAR) (n=3 technical replicates per group. ***p<0.05 vs. LacZ). **(b)** Stable isotope-resolved metabolomics of hiPS-CMs transduced with LacZ or 4F adenovirus: 24 h after transduction, the growth medium was changed to a medium containing 5.5 mM $^{13}C_6$-glucose. After 8 h of incubation with this medium, cellular metabolites were extracted for LC-MS/MS analysis (n=3 technical replicates per group).

Extended Data Fig. 4

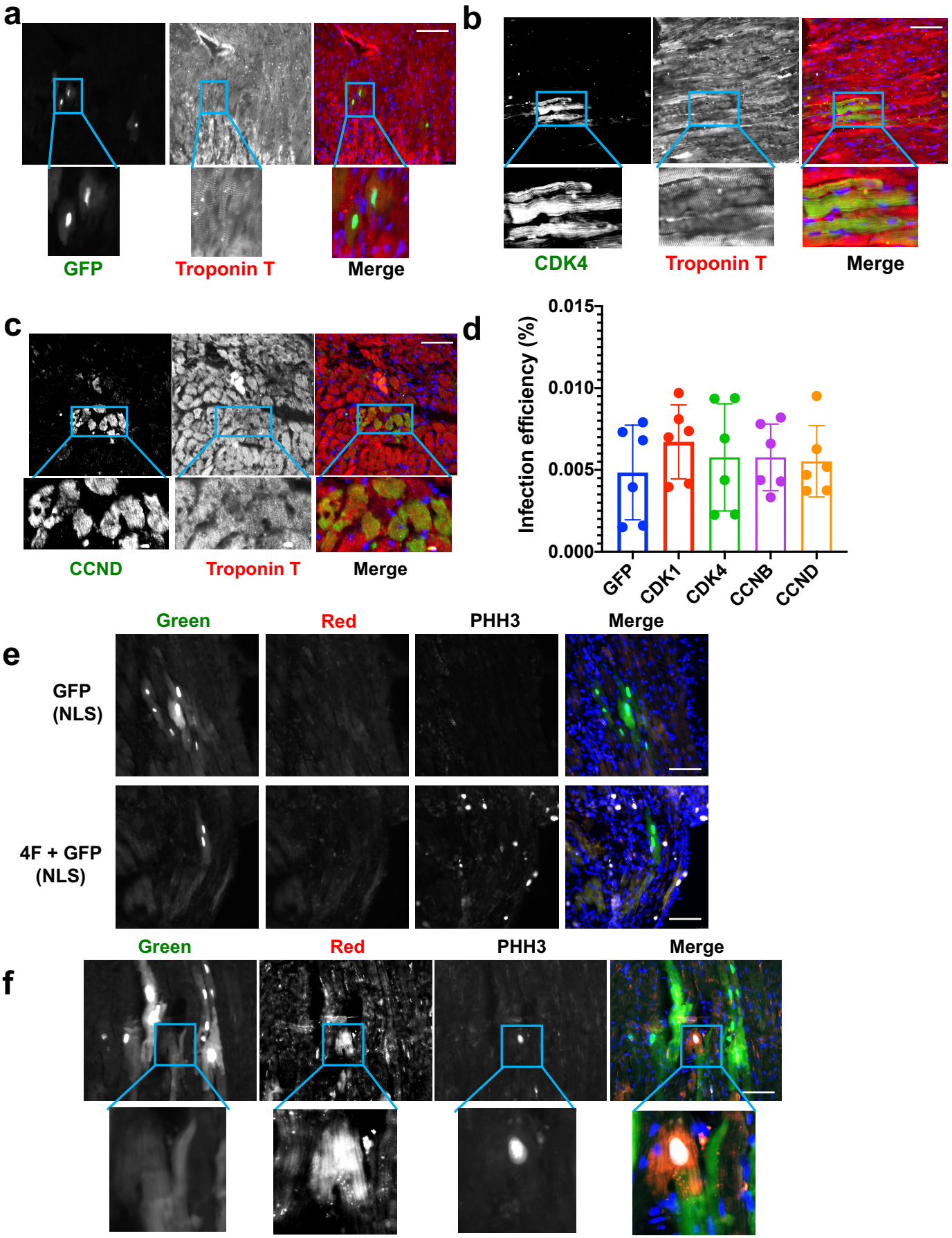

Extended Data Fig. 4. Transient expression of the 4F using modified RNA (modRNA) is not efficient

Representative immunostaining images of C57BL/6 mouse heart sections injected with modRNAs for nuclear GFP (NLS) **(a)**, CDK4 **(b)**, or cyclin D (CCND) **(c)** in citrate sucrose buffer and co-stained with troponin-T antibodies to identify the cardiomyocytes (Scale bar=200μm). **(d)** Bar graph shows the quantification of infection efficiency is <0.01% for GFP, CDK1, CDK4, CCNB, and CCND (6 animals in each group). **(e)** Representative immunostaining images of a-MHC-MADM mouse heart sections injected with modRNAs for nuclear GFP (NLS) (upper panel) or 4F + nuclear GFP (lower panel) in citrate sucrose buffer and co-stained with pHH3 antibodies to identify the proliferating cells. Due to the low infection efficiency of the modRNA, we co-injected nuclear GFP to identify the location of the injection (Scale bar=100μm). **(f)** Immunostaining of α-MHC-MADM mouse heart sections injected with modRNAs for 4F + nuclear GFP in citrate sucrose buffer and co-stained with pHH3 antibodies to identify the proliferating cells. The magnified cardiomyocyte is mononucleated, single-colored, and positive for pHH3, which indicates a cardiomyocyte proliferation event at the injection site as marked by the nuclear GFP (only 10-15 events of single-colored cardiomyocytes were noticed/mouse heart due to the low infection efficiency).

Extended Data Fig. 5

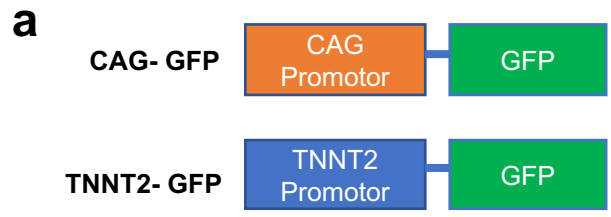

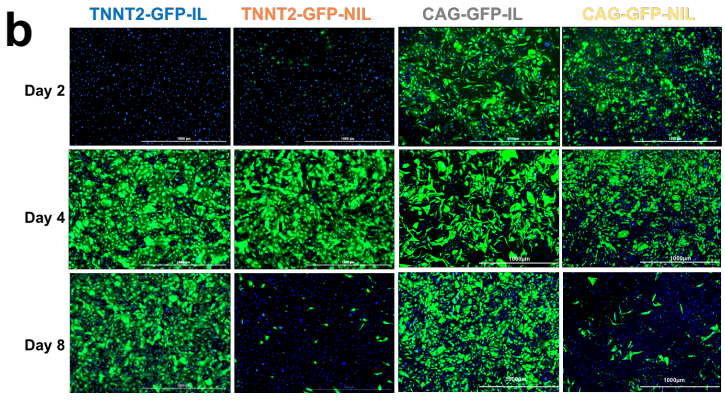

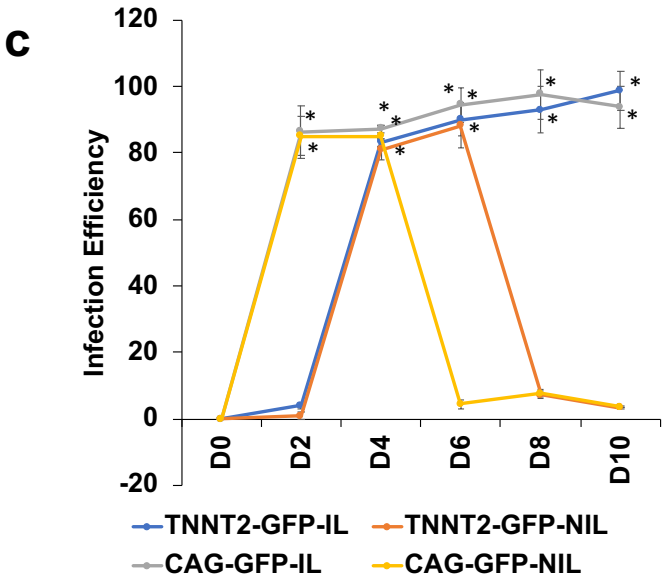

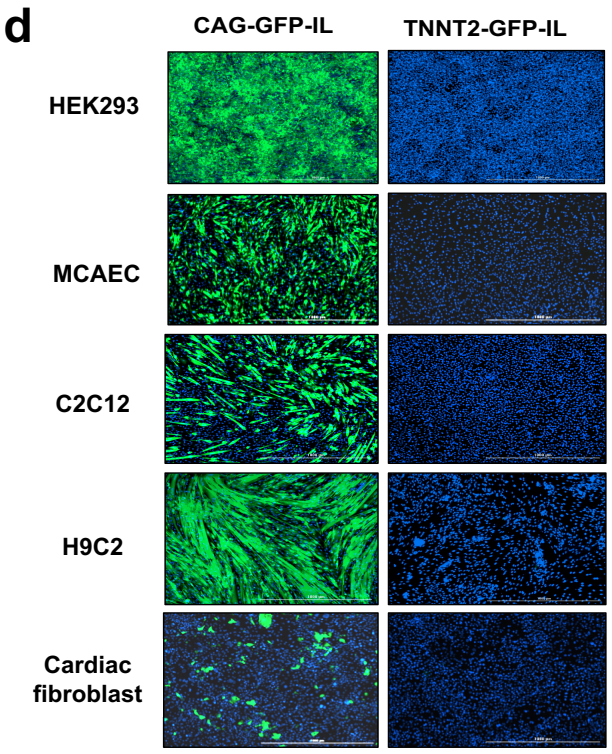

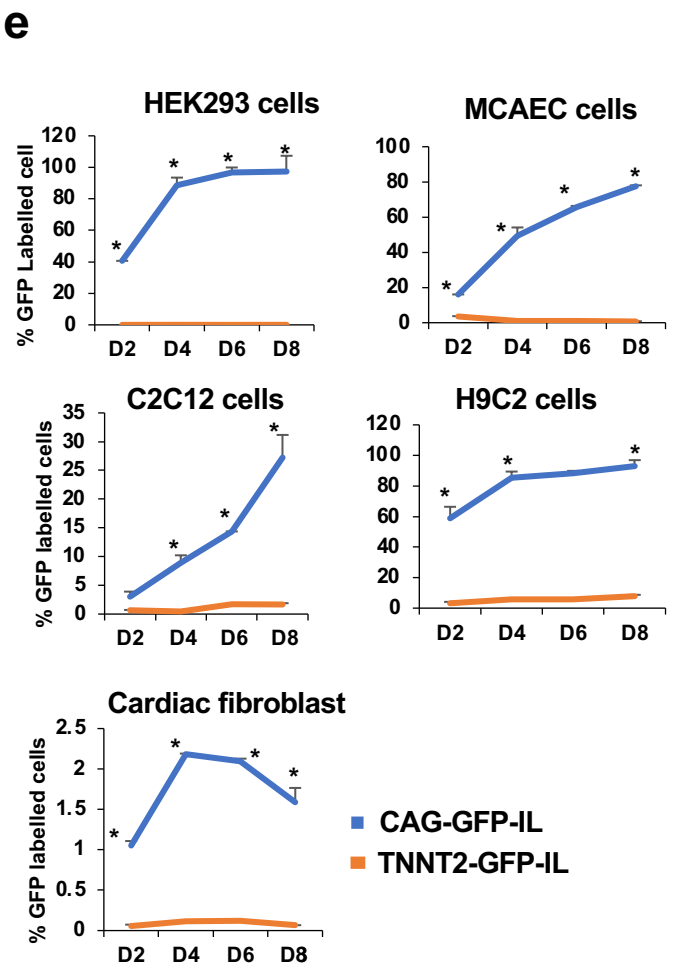

Extended Data Fig. 5. TNNT2 promoter does not drive the protein expression in other cell types.
(a) Schematic diagram of the plasmid design. **(b)** Representative live-cell images of hiPS-CMs treated with TNNT2-GFP-IL, TNNT2-GFP-NIL, CAG-GFP-IL, or CAG-GFP-NIL for 2, 4, 8 days (Scale bar=1000μm). **(c)** Quantification of GFP expression per 100 nuclei (or infection efficiency) (n=3 independent experiments conducted in duplicate, *P<0.05 vs. day 0 expression). **(d)** Representative live-cell images to show GFP expression (green) and nuclei (blue) in kidney cells (HEK293), mouse coronary artery endothelial cells (MCAEC), muscle cells (H9C2 and C2C12 myoblasts), and cardiac fibroblasts infected with CAG-GFP-IL (left panel) or TNNT2-GFP-IL (right panel) for four days (Scale bar= 1000μm). **(e)** Quantification of GFP expression per 100 nuclei for 2, 4, 6, or 8 days post-infection. (n=2 independent experiments conducted in duplicate, *p<0.05 compared to TNNT2-GFP-IL)

Extended Data Fig. 6

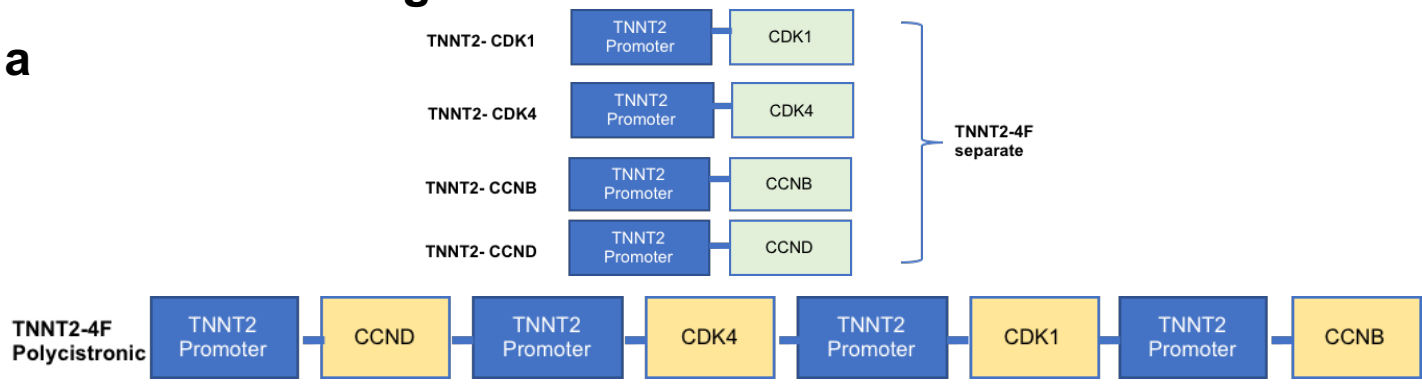

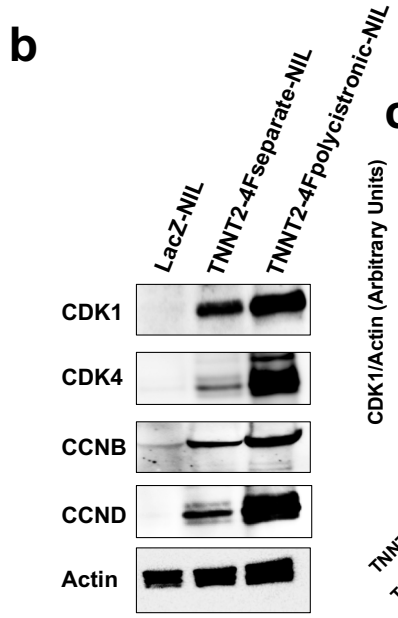

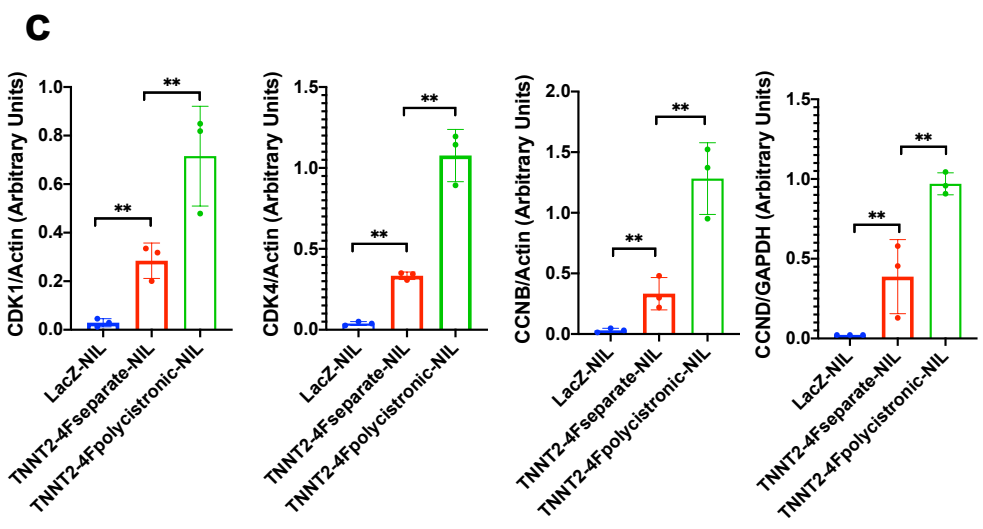

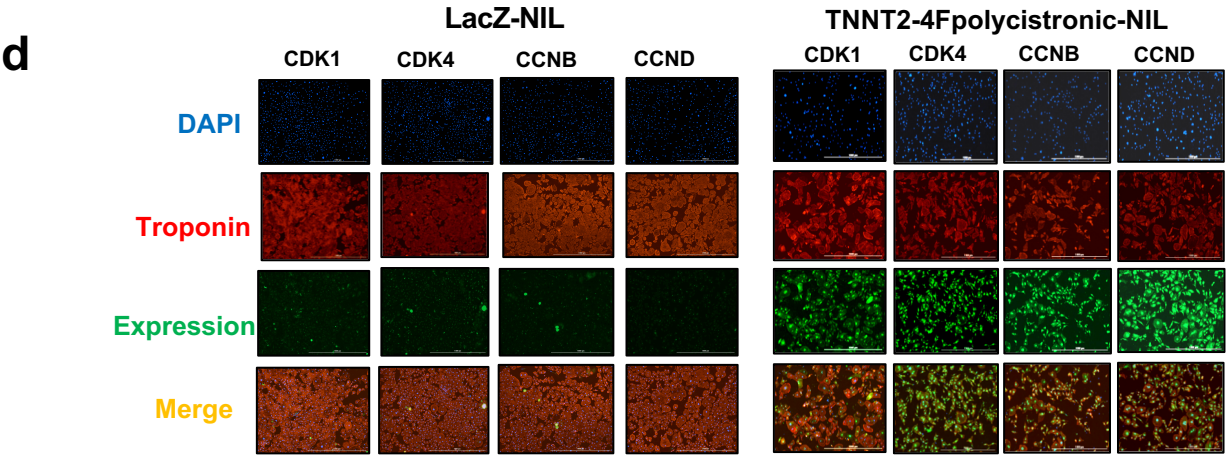

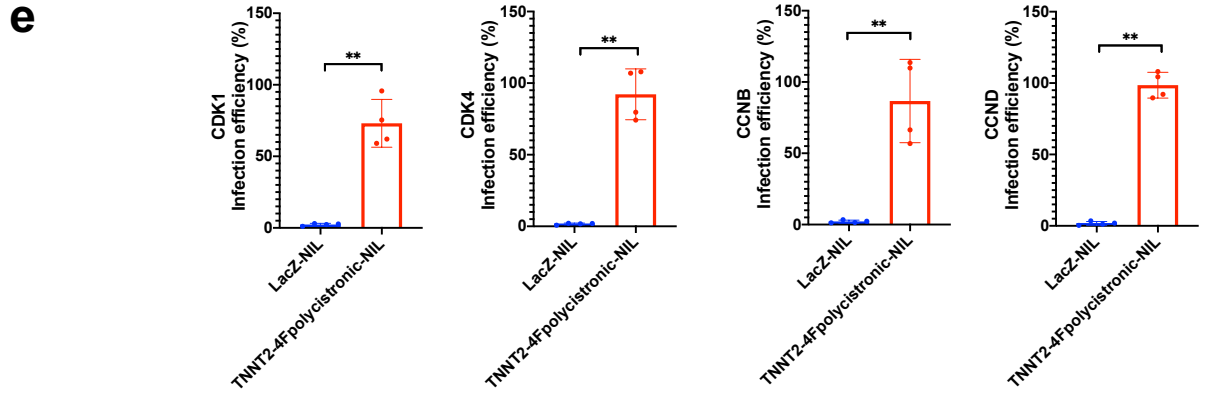

Extended Data Fig. 6. TNNT2-4Fpolycistronic-NIL efficiently drives 4F protein expression in hiPS-CMs

(a) Schematic diagram of the plasmid design for TNNT2-4Fseparate (Top panel) and TNNT2-4F polycistronic (Bottom panel). **(b)** Representative Western blots from protein lysates of hiPS-CMs treated with LacZ-NIL, TNNT2-4Fseparate-NIL, or TNNT2-4Fpolycistronic-NIL for four days to demonstrate the protein expression of the cell cycle factors. **(c)** Quantification of the protein expression of each cell cycle factor (n=3 independent experiment, **p<0.01 compared to the LacZ-NIL control group). **(d)** Representative images of hiPS-CMs treated with LacZ-NIL, or TNNT2-4Fpolycistronic-NIL for four days and stained with antibody against troponin-T (red), or the specified cell cycle factor protein expression (green) (Scale bar=1000μm). **(e)** Quantification of the infection efficiency of each cell cycle factor (n=2 independent experiment conducted in duplicate, **p<0.01 compared to the LacZ-NIL control group).

Extended Data Fig. 7

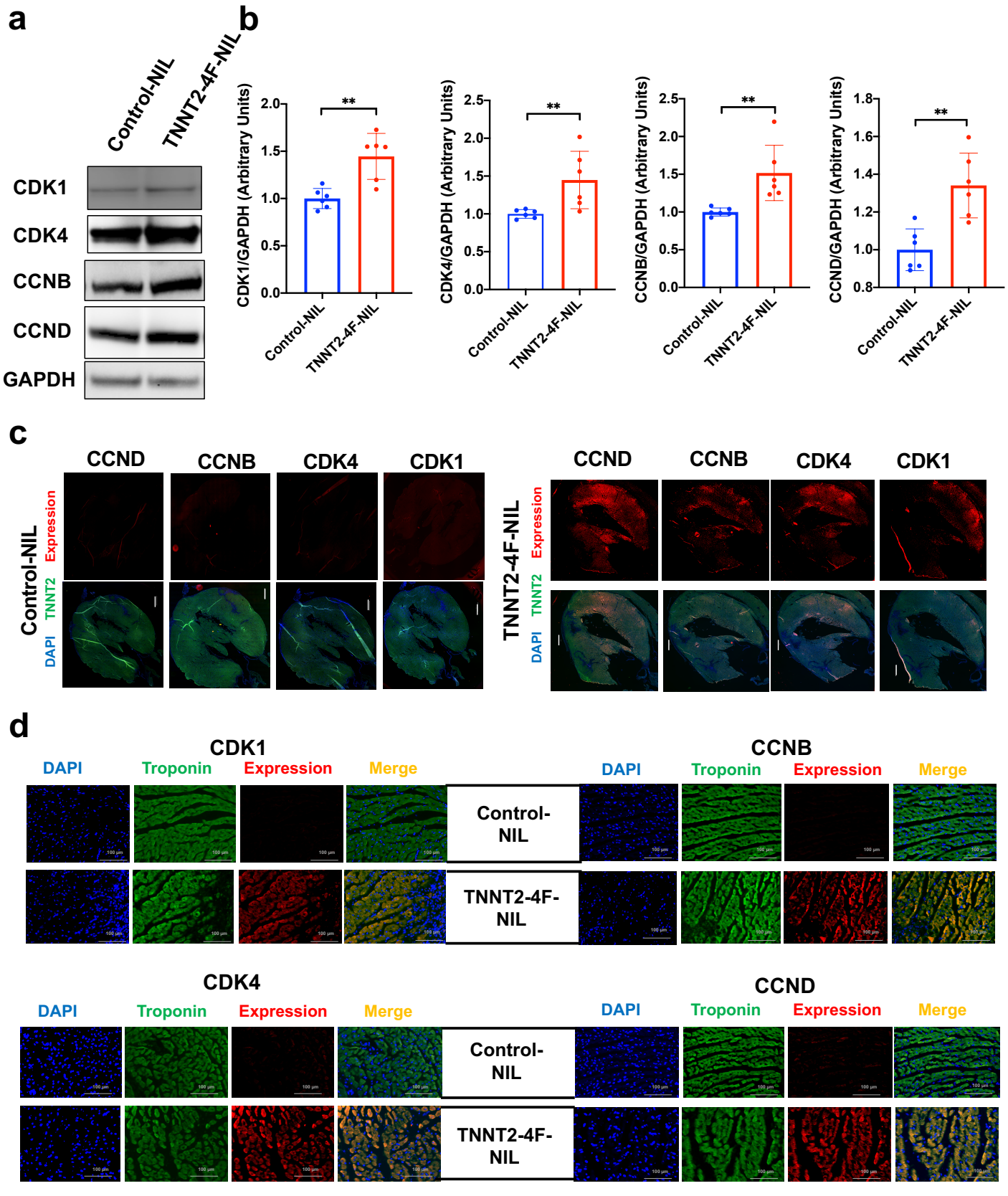

Extended Data Fig. 7. TNNT2-4F-NIL drives significant 4F expression in rat hearts *in vivo* six days post-injection

(a) Representative Western blots from protein lysates of rat heart injected with TNNT2-GFP-NIL (Control-NIL), or TNNT2-4Fpolycistronic-NIL (TNNT2-4F-NIL) and harvested after six days to demonstrate the cell cycle factors' protein expression. **(b)** Quantification of the protein expression of each cell cycle factor (n=3 animals in each group done in duplicates, **p<0.01 compared to the LacZ-NIL control group). **(c)** Representative images of the whole section of rat hearts (Scale bar=1mm) or **(d)** zoom-in higher magnification at the injected site (Scale bar=100μm) collected six days following intramyocardial injection of TNNT2-4F-NIL or control NIL and stained for troponin-T (green), DAPI (Blue), and red for CDK1, CDK4, CCNB or CCND.

Extended Data Fig. 8

a

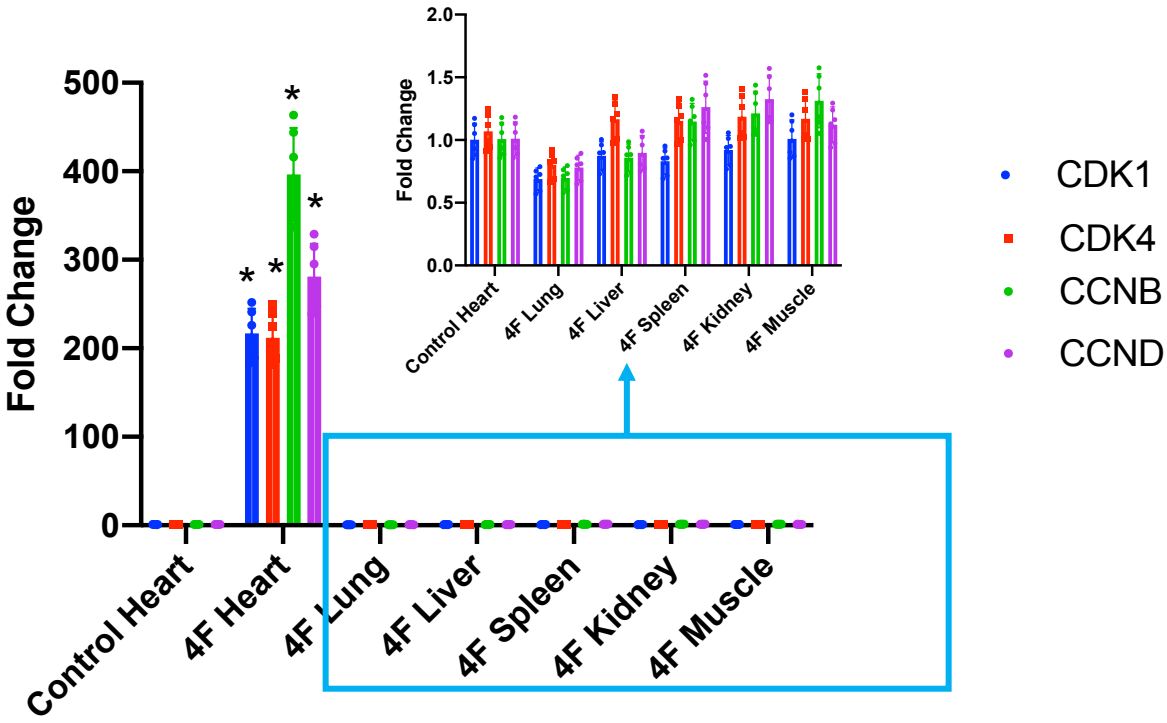

Extended Data Fig. 8. Intramyocardial injection of TNNT2-4Fpolycistronic-NIL drives human CDK1, CDK4, CCNB, CCND expression specifically in the rat hearts

(a) Bar graph shows qRT-PCR quantification for human gene expression of the four cell cycle genes in different tissues from rats six days after intramyocardial injection of TNNT2-4Fpolycistronic-NIL or control TNNT2-GFP-NIL (n=3 animal per group each in duplicate, *p<0.05 compared to the control group).

Extended Data Fig. 9

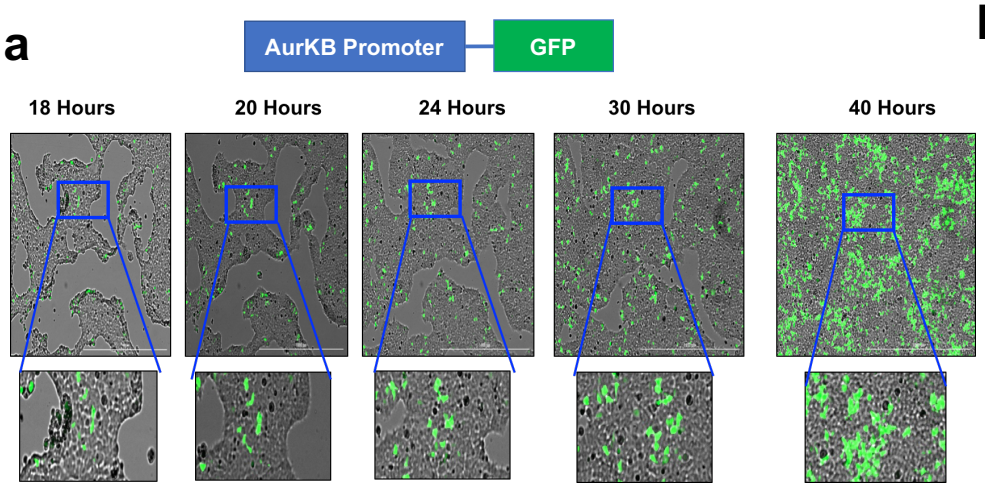

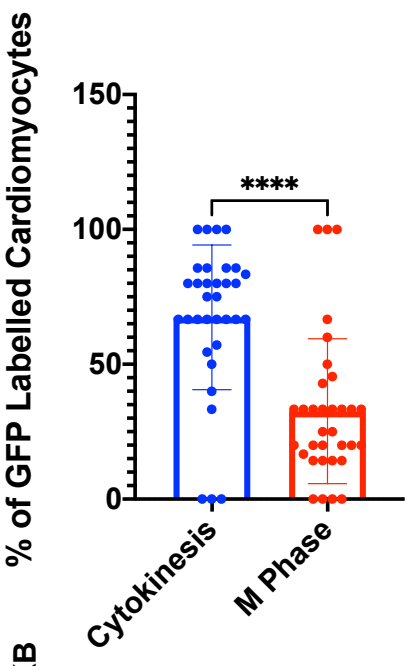

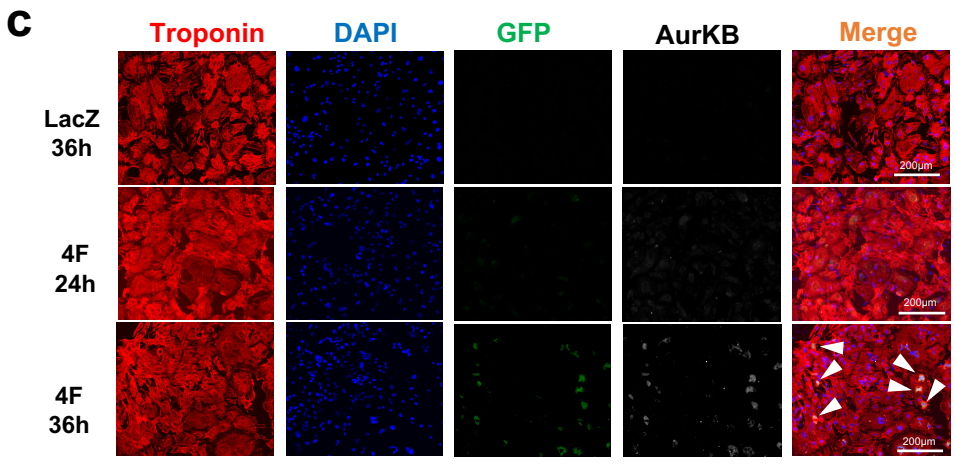

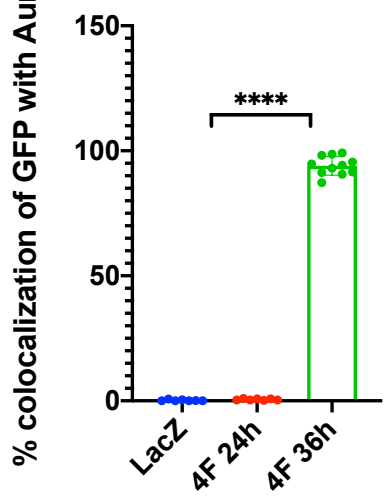

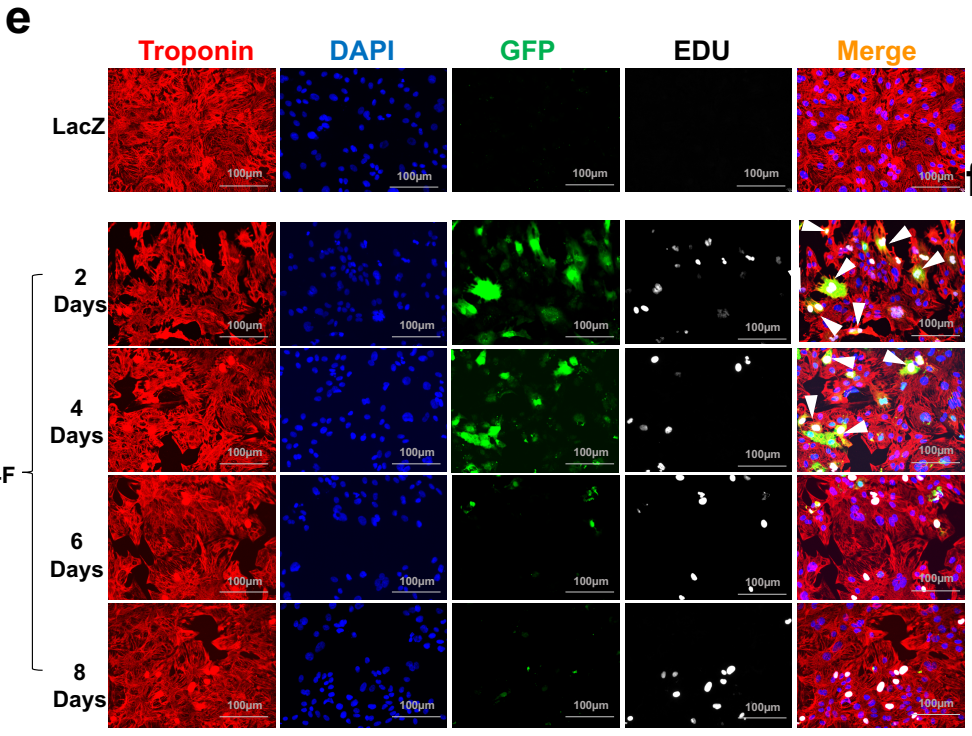

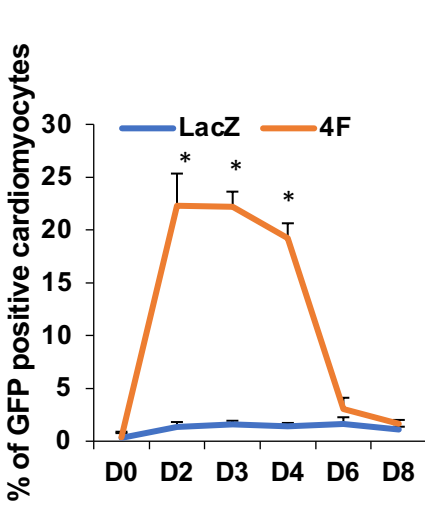

Extended Data Fig. 9. AurKB-GFP is a novel mitosis marker *in vitro*

(a) Schematic diagram of the AurKB-GFP construct and representative live-cell images of HEK293 cells treated with AurKB-GFP-IL (Scale bar=1000μm). **(b)** Quantification of live video images of GFP positive hiPS-CMs that visually completed cytokinesis (200 cells analyzed from in each group from 2 independent experiments, a total of 33 videos analyzed, ***p<0.001). **(c)** Representative images of hiPS-CMs treated with LacZ or 4F adenovirus and AurKB-GFP-IL for 24, 36 hours and stained with antibody against troponin-T (red), GFP (green), and Aurora kinase B protein (AurKB) (gray) (Scale bar 200μm). **(d)** Quantification of the colocalization of GFP positive cardiomyocytes with the AurKB protein (n=3 independent experiments conducted in triplicate, ***p<0.001 compared to LacZ). **(e)** Representative images of hiPS-CMs treated with LacZ or 4F adenovirus and AurKB-GFP-IL for 2, 4, 6, and 8 days and stained with antibody against troponin-T (red), GFP (green), and EDU (gray) (Scale bar 100μm). **(f)** Quantification of the percentage of GFP positive cardiomyocytes (n=2 independent experiments conducted in triplicate, *p<0.05 compared to D0).

Extended Data Fig. 10

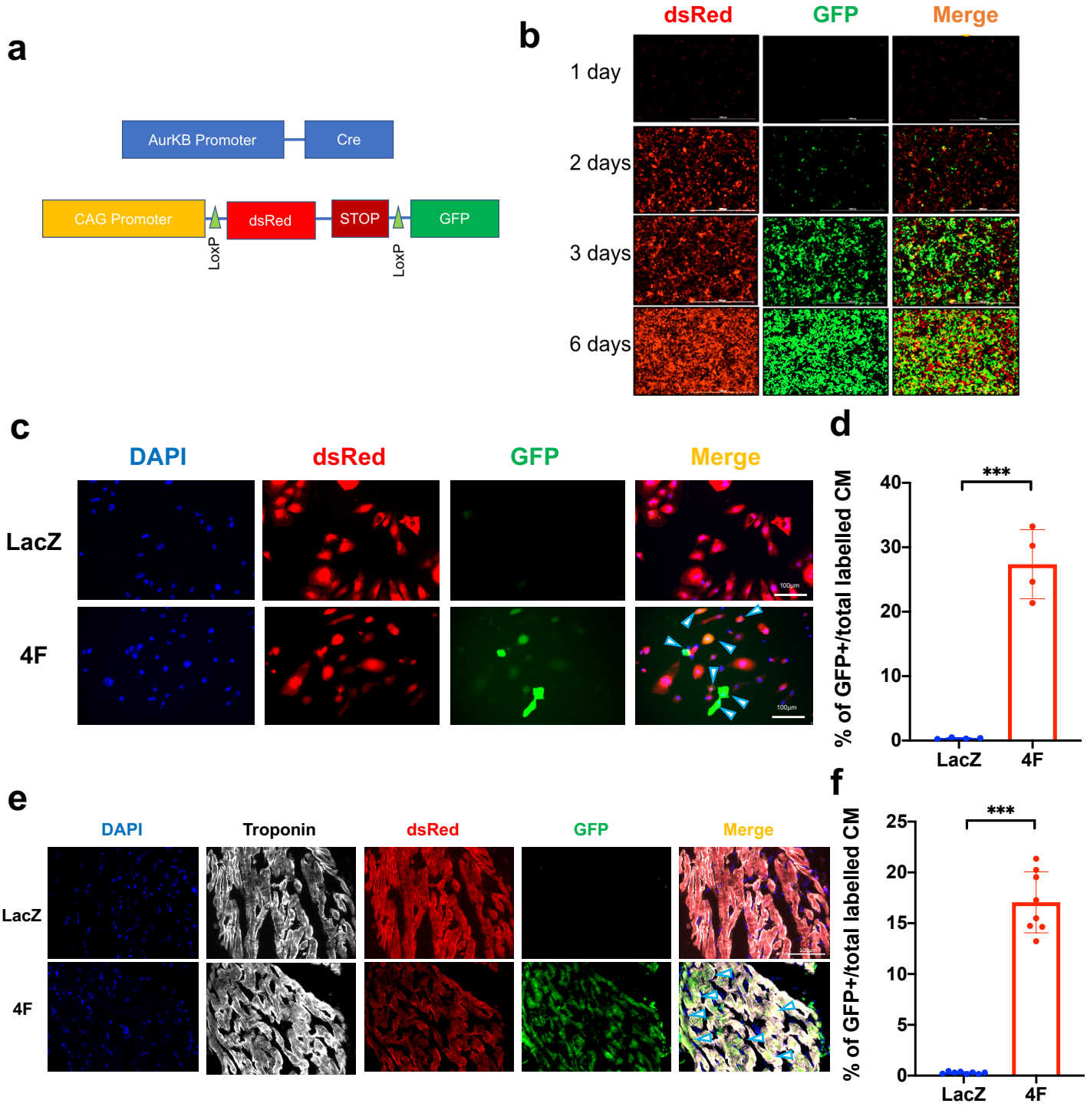

Extended Data Fig. 10. Double reporter system to track mitosis events based on the AurKB promoter

(a) Schematic diagram of the double reporter system vectors design. **(b)** Live images of HEK293 cells treated with the double reporter system over time, showing the switch between red and green color during proliferation (Scale bar=1000μm). **(c)** Representative images of live hiPS-CMs treated with LacZ or 4F adenovirus and the double reporter system for 48 h. Live cell DAPI was added to label the nuclei. Arrows point to cardiomyocytes with color switch following proliferation (Scale bar=100μm). **(d)** Quantification of the percentage of GFP positive cells (n=4 independent experiments each in duplicate, ***p<0.001 vs. LacZ control group). **(e)** Representative images of pig heart slices treated with LacZ or 4F adenovirus and double reporter system-IL for four days. Arrows point to cardiomyocytes with color switch following proliferation (Scale bar=100μm). **(f)** Quantification of the percentage of GFP positive cells (n=4 independent heart slices each in duplicate, ***p<0.001 vs. LacZ control group).

Extended Data Fig. 11

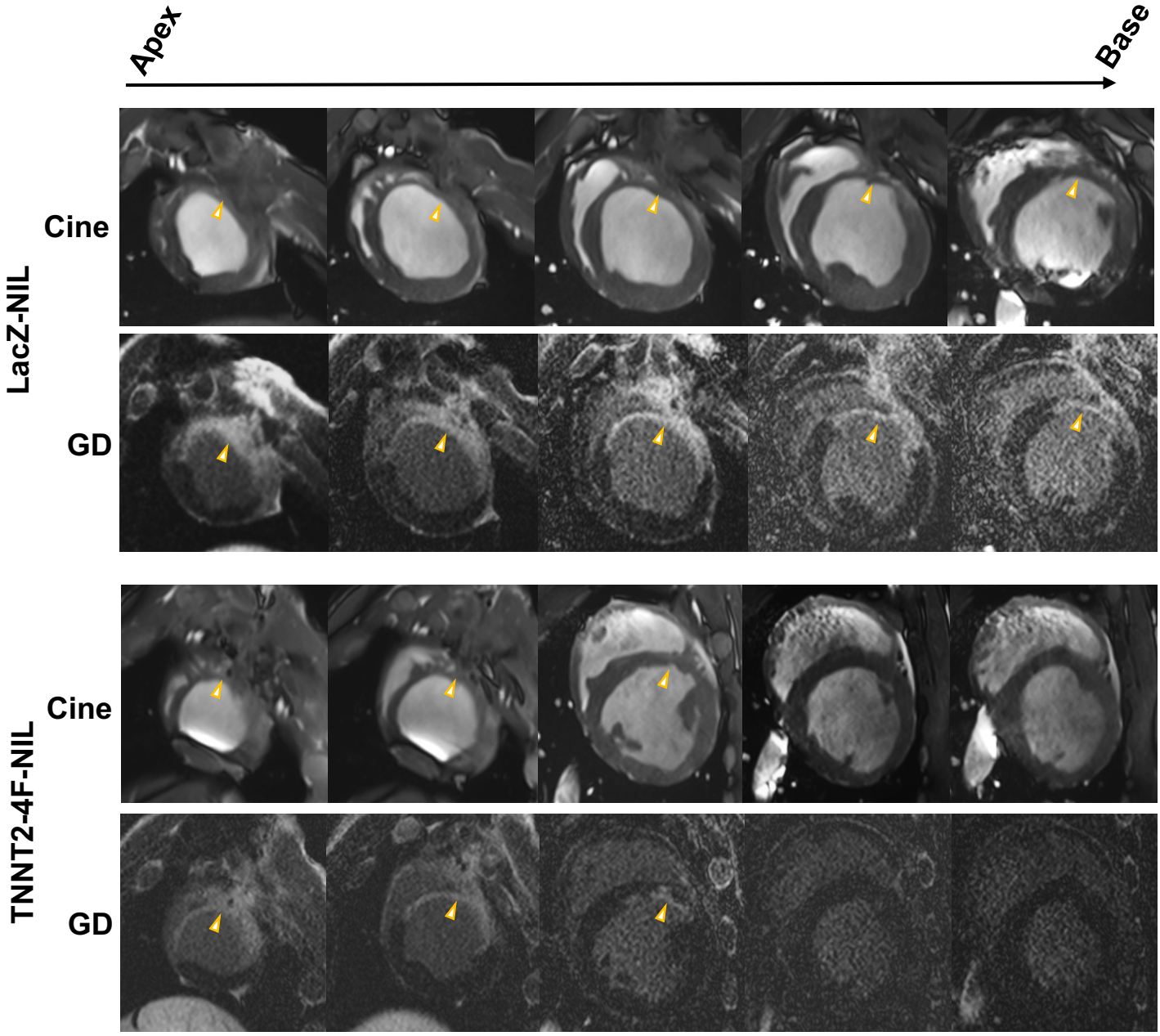

Extended Data Fig. 11. Representative magnetic resonance images of porcine hearts four weeks post-treatment

Representative cross-section magnetic resonance images (MRI) 4 weeks after viral injection before (cine) and after gadolinium enhancement of the scar (GD) shows ventricular wall thinning in cine mode and white scar tissue in GD mode at the infarct site in the control group with significant improvement in animals that received the TNNT2-4F-NIL (arrows). Multiple images from the bottom (apex) to the top of the ventricular chambers (base) are shown.